our study, only the very weak perchlorate ligand is available for coordination and products are relatively unstable.

Conclusions

The lability of mercury dithiocarbamate complexes exerts considerable influence in the mass spectrometry, NMR, and electrochemical experiments. In mass spectrometry and NMR spectrometry, rapid dimer formation appears to be responsible for the observation of exchange process. The lability of the mercury(II) complexes and their rapid interactions with elemental mercury and mercury(I) together with dimer formation also influences the nature of electrode process occurring at mercury electrodes.

Acknowledgment. Financial assistance from the Australian Research Grants Scheme is gratefully acknowledged as is technical assistance in the area of mass spectrometry from G. R. Franklin and discussion on the electrochemistry with K. Hanck.

Appendix of Symbols and Abbreviations

E	potential
i	current
$E_{1/2}$	half-wave potential—defined by $i = {}^1/_2 i_d$
$E_{1/4}-E_{3/4}$	difference in potential between $i = {}^1/_4 i_d$ and $i = {}^3/_4 i_d$
i_d	limiting diffusion-controlled current
E_p	peak position
i_p	peak current
dc	direct current
ΔE_p	separation in forward and reverse scan potentials in cyclic voltammetry
$w_{1/2}$	differntial-pulse polarogram peak width at peak half-height
E_p^{red}	peak potential for reduction in cyclic voltammetry
E_p^{ox}	peak potential for oxidation in cyclic voltammetry
NMR	nuclear magnetic resonance
δ	NMR chemical shift
m/e	mass to charge ratio
average δ	arithmetic average $[\delta(HgL_2) + \delta(HgL'_2)]/2$
mixed δ	experimentally observed shift for approximately equal concentrations of HgL_2 and HgL'_2
dtc	dithiocarbamate
L	RR'dtc ligand
Me	methyl
Et	ethyl
i-Pr	isopropyl
n-Bu	*n*-butyl
i-Bu	isobutyl
t-Bu	*tert*-butyl
c-Hx	cyclohexyl
Ph	phenyl
pipdtc	piperidine-*N*-carbodithioate
2-Mepipdtc	2-methylpiperidine-*N*-carbodithioate
3-Mepipdtc	3-methylpiperidine-*N*-carbodithioate
4-Mepipdtc	4-methylpiperidine-*N*-carbodithioate
2,6-dimepipdtc	2,6-dimethylpiperidine-*N*-carbodithioate
pyrrdtc	pyrrolidine-*N*-carbodithioate
morphdtc	morpholine-*N*-carbodithioate

Registry No. $Hg(Me_2dtc)_2$, 15415-64-2; $Hg(Et_2dtc)_2$, 14239-51-1; $Hg(i\text{-}Pr_2dtc)_2$, 21439-57-6; $Hg(n\text{-}Bu_2dtc)_2$, 21439-58-7; $Hg(i\text{-}Bu_2dtc)_2$, 79001-48-2; $Hg(n\text{-}Hx_2dtc)_2$, 21439-60-1; Hg(Me,*n*-Budtc)$_2$, 91003-05-3; Hg(Et,*n*-Budtc)$_2$, 79572-82-0; Hg(*n*-Bu,*t*-Budtc)$_2$, 79572-80-8; $Hg(c\text{-}Hx_2dtc)_2$, 21439-59-8; Hg(Me,Phdtc)$_2$, 79572-86-4; Hg(Et,Phdtc)$_2$, 78320-43-1; Hg(*i*-Pr,Phdtc)$_2$, 91003-06-4; Hg(pipdtc)$_2$, 21439-62-3; Hg(2-Mepipdtc)$_2$, 79572-81-9; Hg(3-Mepipdtc)$_2$, 79572-84-2; Hg(4-Mepipdtc)$_2$, 79572-85-3; Hg(2,6-dimepipdtc)$_2$, 79594-68-6; Hg(morphdtc)$_2$, 14024-75-0; Hg(pyrrdtc)$_2$, 41060-60-0; Hg(*n*-Pedtc)$_2$, 91003-07-5; Hg, 7439-97-6; ^{199}Hg, 14191-87-8.

Contribution from the Department of Chemistry, Brookhaven National Laboratory, Upton, New York 11973

Ground- and Excited-State Electron-Transfer Reactions: Photoinduced Redox Reactions of Poly(pyridine)ruthenium(II) Complexes and Cobalt(III) Cage Compounds

CHUP-YEW MOK, ANDREW W. ZANELLA, CAROL CREUTZ, and NORMAN SUTIN*

Received September 13, 1983

Rate constants for the quenching of poly(pyridine)ruthenium(II) (RuL_3^{2+}) excited states by caged cobalt(III) amine complexes ($Co(cage)^{3+}$) range from 2×10^8 to 1×10^9 M^{-1} s^{-1} at 25 °C. The quenching process involves parallel energy transfer ($k_{en} \sim 1 \times 10^8$ M^{-1} s^{-1}) and electron transfer ($k_{el} = (0.1\text{–}1) \times 10^9$ M^{-1} s^{-1}) from $*RuL_3^{2+}$ to $Co(cage)^{3+}$. The rate constants for electron-transfer quenching are consistent with expectations based on an adiabatic semiclassical model. The yields of electron-transfer products range from 0.3 to 1.0, increasing as the rate constants for the back-reaction of RuL_3^{3+} with $Co(cage)^{2+}$ diminish. The relatively low magnitudes of the back-reaction rate constants, $(0.08\text{–}8) \times 10^8$ M^{-1} s^{-1}, are consistent with the high yields of electron-transfer products and derive from poor coupling of the RuL_3^{3+} and $Co(cage)^{2+}$ orbitals.

The redox properties of tris(2,2′-bipyridine)ruthenium(II) and its derivatives are currently being extensively investigated.[1] The reasons for this widespread interest include the use of these complexes as sensitizers in water photodecomposition studies,[1,2] as powerful reductants or oxidants to generate and characterize other reactive species,[3] and as probes of fundamental aspects of electron-transfer processes.[4]

The reduction potentials of the luminescent excited states of the RuL_3^{2+} complexes depend upon the nature of L. By subtle variations in L, the driving force for the redox reactions of $*RuL_3^{2+}$ with a substrate Q may be varied systematically. The change in electron-transfer rate resulting from such free

(1) Sutin, N.; Creutz, C. *Pure Appl. Chem.* **1980**, *52*, 2717. Whitten, D. G. *Acc. Chem. Res.* **1980**, *13*, 83. Kalyanasundaram, K. *Coord. Chem. Rev.* **1982**, *46*, 159.

(2) Balzani, V.; Bolletta, F.; Gandolfi, M. T.; Maestri, M. *Top. Curr. Chem.* **1978**, *75*, 1. Sutin, N. *J. Photochem.* **1979**, *10*, 19. Keller, P.; Moradpour, A.; Amouyal, E.; Kagan, H. B. *Nouv. J. Chim.* **1980**, *4*, 378. Borgarello, E.; Kiwi, J.; Pelizetti, E.; Visca, M.; Grätzel, M. *J. Am. Chem. Soc.* **1981**, *103*, 6324. Kirch, M.; Lehn, J.-M.; Sauvage, J.-P. *Helv. Chim. Acta* **1979**, *62*, 1345. Krishnan, C. V.; Creutz, C.; Mahajan, D.; Schwarz, H. A.; Sutin, N. *Isr. J. Chem.* **1982**, *22*, 98.

(3) (a) Creutz, C.; Keller, A. D.; Sutin, N.; Zipp, A. P. *J. Am. Chem. Soc.* **1982**, *104*, 3618. (b) Krishnan, C. V.; Creutz, C.; Schwarz, H. A.; Sutin, N. *Ibid.* **1983**, *105*, 5617.

(4) Beck, C. R.; Connor, J. A.; Gutierrez, A. R.; Meyer, T. J.; Whitten, D. G.; Sullivan, B. P.; Nagle, J. K. *J. Am. Chem. Soc.* **1979**, *101*, 4815. Balzani, V.; Scandola, F. In "Photochemical Conversion and Storage of Solar Energy"; Connolly, J. S., Ed.; Academic Press: New York, 1981; pp 97–125. Sutin, N.; Creutz, C. *J. Chem. Educ.* **1983**, *60*, 809.

0020-1669/84/1323-2891$01.50/0

Table I. Redox Potentials and Self-Exchange Rates for the $Co(cage)^{3+/2+}$ Couples at 25 °C in 0.20 M Chloride Media

ligand	E°, V	k_{ex}, M^{-1} s^{-1}	ligand	E°, V	k_{ex}, M^{-1} s^{-1}
sepulchrate	−0.32[a]	5.1[a]	$diamsarH_2^{2+}$	−0.01[a,b]	0.024[a]
diamsar	−0.35[b]	0.50[a]	azamesar	−0.34[a]	2.9[a]
$diamsarH^+$	−0.15[b]	~0.1[c]	$ammesarH^+$	−0.19[a]	~0.1[c]

[a] Reference 7. [b] This work. [c] Estimated from the quenching rate constants for the diamsar and $diamsarH^{2+}$ systems, on the assumption of a linear relationship between $\log k_{ex}$ and $z_1 z_2$.

energy variations can yield detailed information about the factors determining the rate of the redox reaction of $*RuL_3^{2+}$ with Q (and of the back-reaction of RuL_3^{3+} with Q^-). Information about the properties of the $Q-Q^-$ couple can also be obtained from these studies. Here we have used this approach to probe the redox properties of cobalt(III) and cobalt(II) cage compounds.

Unlike the reduced forms of the widely studied $Co(NH_3)_5X^{2+}$ complexes, the cobalt(II) cage compounds are fairly inert to substitution.[5] As a consequence, the reductions of the cage compounds are chemically reversible and the redox potentials of the cobalt(III)-(II) couples, as well as the kinetics of the outer-sphere oxidation of cobalt(II) complexes, can be readily determined. In recent years the exchange rates and redox potentials of a variety of cobalt(III/II) cage complexes have been reported by Sargeson and his colleagues.[5-7] Those of relevance to this work are summarized in Table I. Recently the use of cobalt cage compounds as relays in water photoreduction schemes has been proposed and demonstrated.[8,9] The results presented here implicate strong nonadiabaticity in the reactions of RuL_3^{3+} with $Co(cage)^{2+}$ compounds and are pertinent to the use of the cobalt complexes in photoconversion systems.

Experimental Section

Materials. Commercial $[Ru(bpy)_3]Cl_2 \cdot 6H_2O$ (G. F. Smith) was recrystallized from hot water. The preparation and purification of the other poly(pyridine)ruthenium(II) complexes have been described previously.[10] We are indebted to Professor A. M. Sargeson for providing $[Co(azamesar)](ClO_4)_3$, $[Co(diamsarH_2)]Cl_5 \cdot H_2O$, and $[Co(ammesar)]Cl_3$.[6]

[Co(sep)]Cl_3 was prepared by a modification of the method of Harrowfield et al.[11] To a stirred suspension of Li_2CO_3 (12.5 g) and $[Co(en)_3]Cl_3 \cdot H_2O$ (10 g) in water (63 mL) were added aqueous formaldehyde (325 mL, 37%) and aqueous ammonia (300 mL, 16%) concurrently and dropwise from two separatory funnels. The mixture was then stirred for another hour and filtered, and the filtrate was acidified to pH 2 with concentrated $HClO_4$. The solution was sorbed onto an ion-exchange column (Dowex 50W-X2, H^+ form, 200–400 mesh, 3.5 × 10 cm), and a pink species was eluted with sodium citrate solution (1350 mL, 0.2 M). The column was then washed with water and 1 M HCl. Elution with 3 M HCl gave an orange eluate, which was evaporated to dryness on a rotary vacuum evaporator at 50 °C. The compound isolated was recrystallized twice, first from water–acetone and then from dilute HCl; yield 2.1 g. Anal. Calcd for $CoC_{12}H_{30}N_8Cl_3$: H, 6.69; C, 31.91; N, 24.81; Cl, 23.54; Co, 13.05. Found: H, 6.92; C, 30.74; N, 23.29; Cl, 21.1; Co, 12.8. Solutions containing $Co(sep)^{2+}$ and $Co(diamsar)^{2+}$ were prepared by amalgamated zinc reduction of the corresponding cobalt(III) complexes in the medium used for the flash photolysis studies.

Triethanolamine (TEOA, Fisher Certified) was purified by dissolving 15 mL of the amine in 700 mL of absolute ethanol and adding dropwise either concentrated HCl or 6 M H_2SO_4 to the cooled solution. The white precipitate of (TEOAH)Cl or $(TEOAH)_2SO_4$ was collected on a frit, washed with absolute ethanol, and stored in a vacuum desiccator. Anal. Calcd for (TEOAH)Cl: Cl, 19.1. Found: Cl, 18.1. Calcd for $(TEOAH)_2SO_4$: SO_4, 24.2. Found: SO_4, 23.6.

Methylviologen chloride (*N,N'*-dimethyl-4,4'-bipyridinium dichloride) and *N*-ethylmorpholine were used as purchased from Aldrich.

Quenching Rate Constants. Quenching rate constants were determined from Stern–Volmer plots of emission intensity or lifetime data, as described elsewhere.[10] Emission intensity at 600–630 nm was monitored on a thermostated Perkin-Elmer Hitachi spectrofluorimeter. The solutions were deaerated by Ar bubbling for ~20 min and placed in the cell compartment of the spectrofluorimeter for a further 15 min to attain thermal equilibrium (25 °C). The samples were excited at wavelengths around 395 nm where absorption by the Co(III) complexes was minimal: in most cases the correction for Co(III) absorption[12] did not exceed 10%.

Continuous Photolysis. The photolysis train consisted of a 450-W xenon lamp, focusing lenses, a Bausch and Lomb high-intensity monochromator, and a thermostated cell compartment. Solutions containing RuL_3^{2+}, TEOA, and $Co(sep)^{3+}$ (or methylviologen) were bubbled with Ar before irradiation in flat-walled 2 × 2 × 4.5 cm high cells. The solutions were stirred during the photolysis, and the Co(III) concentration was monitored at 473 nm (λ_{ex} = 405 nm) while the formation of methylviologen radicals was monitored at 602 nm (λ_{ex} = 450 nm). The incident light intensity (typically 2×10^{-7} einstein min^{-1}) was determined by $Co(NH_3)_5Cl^{2+}/Ru(bpy)_3^{2+}$ actinometry.[13]

Flash Photolysis. The absorbance changes at 450 nm due to the back-reaction following flash photolysis of deaerated solutions ((1–7) × 10^{-3} M Co(III), (2–5) × 10^{-5} M Ru(II)) were studied by using either a frequency-doubled neodymium laser[10] or a Phase-R Model DL-1100 dye laser.[14] In the latter case, the laser pulse width was ~0.6 μs and the reaction solutions were contained in tightly stoppered 1-cm^2 fluorescence cells fitted with a 0.50-cm slit facing the dye laser and a 0.20-cm slit facing the probe. For $Co(sep)^{3+}-Ru(phen)_3^{2+}$ and $Co(diamsar)^{3+}-RuL_3^{2+}$ the back-reaction rate constants were also determined under pseudo-first-order conditions in the presence of excess $Co(cage)^{2+}$. The final $Co(cage)^{2+}$ concentration was verified by oxidizing the reaction mixture with air and determining the absorbance change at 473 nm.

The yield of separated electron-transfer products Y_{el} was determined with use of the frequency-doubled Nd laser as excitation source. The absorbance changes occurring during and after the 25-ns 530-nm pulse were monitored at 420–450 nm. Quenching in the $RuL_3^{2+}-Fe^{3+}$ system in 0.5 M H_2SO_4 was assumed to produce separated RuL_3^{3+} and Fe^{2+} in 100% yield (Y_{el} = 1.0), and absorbance measurements on this system were used (after correction for fraction unquenched) to calculate the ratio $\Delta\epsilon_{III}/\Delta\epsilon_*$ ($\Delta\epsilon_{III} = \epsilon(RuL_3^{2+}) - \epsilon(RuL_3^{3+})$; $\Delta\epsilon_* = \epsilon(RuL_3^{2+}) - \epsilon(*RuL_3^{2+})$) at the monitoring wavelength used in the Co(cage) experiments. The absorbance changes were similarly measured at the end of the pulse (ΔA_*) and at the end of the excited-state decay (ΔA_{III}) in the presence of $Co(cage)^{3+}$, and the yield of separated electron-transfer products was calculated from $Y_{el} = [(\Delta A_{III})(\Delta\epsilon_*)]/[(\Delta A_*)(\Delta\epsilon_{III})f_q]$ where $f_q = K_{SV}[Q]/(1 + K_{SV}[Q])$ and K_{SV} is the Stern–Volmer constant.

Cyclic Voltammetry. A PAR electrochemistry system consisting of a Model 173 potentiostat and a Model 175 universal programmer was employed. Cyclic voltammograms were recorded on an X-Y recorder with sweep rates of 50 or 100 mV s^{-1}. A three-compartment cell was used. The electrodes consisted of a glassy-carbon working electrode, a Pt-wire counterelectrode, a SCE reference, and a pH minielectrode (Metrohm). Deaerated $Co(diamsarH_2)^{5+}$ solutions (5.0×10^{-3} M in 0.2 M Cl^-, 0.01 M phosphate, 0.01 M acetate, initially at pH 1) at ambient temperature (~22 °C) were blanketed with argon, and small volumes of 0.1 or 2 M NaOH were introduced through a rubber septum with a 1-mL syringe. After the solution was mixed

(5) Creaser, I. I.; Geue, R. J.; Harrowfield, J. M.; Herlt, A. J.; Sargeson, A. M.; Snow, M. R.; Springborg, J. *J. Am. Chem. Soc.* **1982**, *104*, 6016.
(6) Bond, A. M.; Lawrance, G. A.; Lay, P. A.; Sargeson, A. M. *Inorg. Chem.* **1983**, *22*, 2010.
(7) Creaser, I. I.; Sargeson, A. M.; Zanella, A. W. *Inorg. Chem.* **1983**, *22*, 4022.
(8) Houlding, V.; Geiger, T.; Kölle, U.; Grätzel, M. *J. Chem. Soc., Chem. Commun.* **1982**, 681. Scandola, M. A. R.; Scandola, F.; Indelli, A.; Balzani, V. *Inorg. Chim. Acta* **1983**, *76*, L67.
(9) Lay, P. A.; Mau, A. W. H.; Sasse, W. H. F.; Creaser, I. I.; Gahan, L. R.; Sargeson, A. M. *Inorg. Chem.* **1983**, *22*, 2347.
(10) Lin, C.-T.; Böttcher, W.; Chou, M.; Creutz, C.; Sutin, N. *J. Am. Chem. Soc.* **1976**, *98*, 6536. We thank M. Chou for preparing the compounds.
(11) Harrowfield, J. M.; Herlt, A. J.; Sargeson, A. M. *Inorg. Synth.* **1980**, *20*, 85.
(12) Navon, G.; Sutin, N. *Inorg. Chem.* **1974**, *13*, 2159.
(13) Chan, S. F.; Chou, M.; Creutz, C.; Matsubara, T.; Sutin, N. *J. Am. Chem. Soc.* **1981**, *103*, 369.
(14) Hoselton, M. A.; Lin, C.-T.; Schwarz, H. A.; Sutin, N. *J. Am. Chem. Soc.* **1978**, *100*, 2383.

Table II. Rate Constants for the Quenching of $*RuL_3^{2+}$ Emission by $Co(sep)^{3+}$ at 25 °C[a]

ligand, L	$\Delta E_q°$,[b] V	$10^{-8}k_q$,[c] M^{-1} s^{-1} 0.50 M H_2SO_4	0.20 M LiCl
bpy	0.52	2.8	2.9 (3.4[d])
4,4'-$(CH_3)_2$bpy	0.62	4.5	
5-Br(phen)	0.44	2.2	2.8
5-Cl(phen)	0.45	2.0	2.7
phen	0.55	5.5	7.0 (6.3[e])
5-(CH_3)phen	0.58	5.5	7.3
5,6-$(CH_3)_2$phen	0.61	5.7	7.2
4,7-$(CH_3)_2$phen	0.69	7.0	9.5
3,5,6,8-$(CH_3)_4$phen	0.72	3.0	
3,4,7,8-$(CH_3)_4$phen	0.79	6.9	

[a] Medium is 0.50 M H_2SO_4 or 0.20 M LiCl unless otherwise indicated. [b] $\Delta E_q° = E_{Co}° - *E_{Ru}°$ was calculated from the potentials of the $RuL_3^{3+}/*RuL_3^{2+}$ couples given in ref 10 and the potential of the $Co(sep)^{3+/2+}$ couple given in Table I. [c] The values of τ_0 used to calculate k_q were taken from ref 10. The Stern–Volmer constants were determined from emission intensity measurements. [d] Medium is TEOA–LiCl, [TEOA] = 0.2 M, pH 8.1, μ = 0.2 M. [e] Medium is TEOA–LiCl, [TEOA] = 0.1 M, pH 8.1, μ = 0.2 M.

by argon bubbling, the pH was measured and the cyclic voltammogram was recorded (35 traces between pH 1 and 8).

Thermal Reactions. The absorbance increases due to the reaction of $Ru(bpy)_3^{3+}$ with *N*-ethylmorpholine or $Co(diamsar)^{3+}$ at neutral pH were monitored at 450 nm by using a Durrum D-110 stopped-flow spectrophotometer equipped with a 2-cm observation cuvette. The output from the photomultiplier was fed into an on-line computer, and the data were analyzed by nonlinear least-squares fitting program. The slower reactions of $Ru(bpy)_3^{3+}$ were studied at 450 nm on Cary 17 or 210 spectrophotometers. In each case aliquots of freshly prepared solutions of $[Ru(bpy)_3](ClO_4)_3$ in 10^{-3} N H_2SO_4 were mixed with the reductant dissolved in the appropriate medium.

Results

Quenching Rate Constants. The quenching of the emission of the excited states of the poly(pyridine)ruthenium(II) complexes by the cobalt(III) cage compounds and by the other quenchers studied gave good linear relationships (intercept unity) when I_0/I or τ_0/τ was plotted against quencher concentration. The slope of such a plot is the Stern-Volmer constant K_{SV}, and the bimolecular quenching rate constant k_q is obtained from the relationship $k_q = K_{SV}/\tau_0$ where τ_0 is the lifetime of the excited state in the absence of quencher. The values of k_q for $Co(sep)^{3+}$ quenching of the $*RuL_3^{2+}$ emission are presented in Table II, which also contains values of the driving force for the quenching reaction $\Delta E_q°$ calculated from the difference in the redox potentials of the two couples. The quenching rate constants are generally about 30% higher in 0.20 M LiCl than in 0.50 M H_2SO_4, and the rate constant for quenching of $*Ru(bpy)_3^{2+}$ emission by $Co(sep)^{3+}$ is in good agreement with the values determined earlier[8] under somewhat different conditions.

Values of k_q and $\Delta E_q°$ for quenching by $Co(azamesar)^{3+}$, $Co(ammesarH)^{4+}$, $Co(diamsar)^{3+}$, and $Co(diamsarH_2)^{5+}$ in various media are summarized in Table III. In the quenching by $Co(diamsar)^{3+}$, the pH was adjusted to 7.5–8.3 with 0.05 M *N*-ethylmorpholine buffer (pK = 7.67): no quenching by *N*-ethylmorpholine was detected. In some instances k_q values were also determined from emission lifetime measurements made on the solutions used for the cage-escape determinations; these values agreed with the emission intensity values to within 20%.

Continuous Photolysis. The procedure for determining the quantum yield for the formation of $Co(sep)^{2+}$ depended upon measuring the small absorbance decrease at 473 nm (an absorbance maximum of the Co(III) complex) accompanying the reduction of $Co(sep)^{3+}$ to $Co(sep)^{2+}$ ($\Delta\epsilon$ = 97). In order

Table III. Rate Constants for the Quenching of $*RuL_3^{2+}$ Emission by $Co(azamesar)^{3+}$, $Co(ammesarH)^{4+}$, $Co(diamsar)^{3+}$, and $Co(diamsarH_2)^{5+}$ at 25 °C and 0.20 M Ionic Strength[a]

ligand, L	quencher	$\Delta E_q°$,[b] V	$10^{-8}k_q$, M^{-1} s^{-1}
5-Br(phen)	$Co(azamesar)^{3+}$	0.42	2.0
phen	$Co(azamesar)^{3+}$	0.53	4.0
4,7-$(CH_3)_2$phen	$Co(azamesar)^{3+}$	0.67	8.4
5-Cl(phen)	$Co(ammesarH)^{4+}$	0.58	2.3[c]
phen	$Co(ammesarH)^{4+}$	0.68	5.2[c]
4,7-$(CH_3)_2$phen	$Co(ammesarH)^{4+}$	0.82	7.4[c]
5-Br(phen)	$Co(diamsar)^{3+}$	0.41	1.5[d]
5-Cl(phen)	$Co(diamsar)^{3+}$	0.42	1.4[d]
phen	$Co(diamsar)^{3+}$	0.52	3.4[d]
4,7-$(CH_3)_2$phen	$Co(diamsar)^{3+}$	0.66	5.8[d]
5-Br(phen)	$Co(diamsarH_2)^{5+}$	0.75	5.9[c]
phen	$Co(diamsarH_2)^{5+}$	0.86	8.6[c]
4,7-$(CH_3)_2$phen	$Co(diamsarH_2)^{5+}$	1.00	10.6[c]

[a] Ionic strength maintained with LiCl. [b] See footnote b, Table II. The potentials of the cobalt couples are given in Table I. [c] Medium is 0.10 M HCl, 0.10 M LiCl. [d] Medium is 0.16 M LiCl, 0.05 M *N*-ethylmorpholine, pH 7.5.

to establish the validity of the method, a solution containing 7.3×10^{-3} M $Co(sep)^{3+}$, 5.4×10^{-5} M $Ru(bpy)_3^{2+}$, and 0.1 M TEOA (pH 8.1, μ = 0.2 M) was deaerated with Ar in a 2×2 cm cell and irradiated at 405 nm until reduction of 10% of the $Co(sep)^{3+}$ had occurred, as estimated from the absorbance decrease at 473 nm. The cobalt species were then separated from the $Ru(bpy)_3^{2+}$ on a SEP-PAK cartridge in a glovebag under nitrogen. The absorbance of the solution containing the cobalt fraction was then measured at 473 nm and compared with that of an unphotolyzed solution that had been treated in the same manner. The absorbance changes resulting from the photolysis measured for the separated and unseparated solutions were the same within 5%, confirming that the absorbance change at 473 nm measured directly for the photolyzed solution was indeed due to the reduction of $Co(sep)^{3+}$.

The quantum yield for the formation of $Co(sep)^{2+}$ in the $Ru(bpy)_3^{2+}$–$Co(sep)^{3+}$–TEOA system determined by the above procedure was 0.74 ± 0.14 in 0.2 M TEOA, pH 8.1, μ = 0.2 M (LiCl). As a further check of the method, the quantum yield for the formation of MV^+ radical was also determined. Quantum yields of 0.36 ± 0.08 in the above medium and 0.40 ± 0.08 in 0.2 M TEOA, pH 8.1, μ = 0.3 M (Li_2SO_4), were obtained. These values may be compared with the cage-escape yields of 0.25 ± 0.05 (0.17 M Na_2SO_4)[13] and 0.21 (0.2 M Na_2SO_4, 0.5 M NaCl, or 0.5 M H_2SO_4)[15] reported for the MV^+ in flash photolysis studies of the $Ru(bpy)_3^{2+}$–MV^{2+} system. The values for the MV^{2+} system are seen to be in good agreement once a small medium effect and the factor of 2 difference between the cage escape and MV^+ radical yields are considered.[16]

Back-Reaction Rate Constants and Cage-Escape Yields. The absorbance changes accompanying the flash photolysis of the RuL_3^{2+}–$Co(cage)^{3+}$ solutions occur in three stages:

$$RuL_3^{2+} \overset{h\nu}{\rightleftharpoons} *RuL_3^{2+} \quad (1)$$

$$*RuL_3^{2+} + Co(cage)^{3+} \xrightarrow{k_q} RuL_3^{3+} + Co(cage)^{2+} \quad (2)$$

$$RuL_3^{3+} + Co(cage)^{2+} \xrightarrow{k_t} RuL_3^{2+} + Co(cage)^{3+} \quad (3)$$

The first two stages (<1 μs) comprise a net bleaching at 450 nm due to the conversion of RuL_3^{2+} to RuL_3^{3+}. In the third

(15) Kalyanasundaram, K.; Neumann-Spallart, M. *Chem. Phys. Lett.* **1982**, *88*, 7.

(16) Note that the quantum yields for formation of bipyridine radical ions reported in ref 3a have been corrected by the stoichiometric factor 2 and are cage-escape yields.

Table IV. Yields of Separated Electron-Transfer Products and Rate Constants for the Back-Reaction of RuL_3^{3+} with $Co(sep)^{2+}$, $Co(diamsar)^{2+}$, and $Co(diamsarH_2)^{4+}$ at 25 °C and 0.20 M Ionic Strength[a]

ligand, L	Co(II) complex	ΔE_t°,[b] V	$10^{-8}k_t$, M^{-1} s^{-1}	Y_{el}[c]
5-Cl(phen)	$Co(sep)^{2+}$	1.68	8.2	0.35
phen	$Co(sep)^{2+}$	1.58	6.4	0.53
4,7-$(CH_3)_2$phen	$Co(sep)^{2+}$	1.41	5.4	0.64
bpy	$Co(sep)^{2+}$	1.58	5.5	0.51[d]
5-Cl(phen)	$Co(diamsar)^{2+}$	1.71	1.7[e]	0.30[e]
phen	$Co(diamsar)^{2+}$	1.61	0.96[f]	0.65[f]
4,7-$(CH_3)_2$phen	$Co(diamsar)^{2+}$	1.44	0.31[f]	0.90[f]
phen	$Co(diamsarH_2)^{4+}$	1.27	0.079[g]	1.0[g]

[a] Ionic strength maintained with LiCl. [b] $\Delta E_t^\circ = E_{Ru}^\circ - E_{Co}^\circ$ was calculated from the potentials of the RuL_3^{3+}/RuL_3^{2+} couples given in ref 10 and the potentials of the cobalt couples given in Table I. [c] Yield of separated electron-transfer products produced in the quenching reaction corrected for the fraction of $*RuL_3^{2+}$ unquenched by $Co(cage)^{3+}$. The uncertainty in the yields is ±10%. [d] The value of (0.74 ± 0.14)/2 was determined by continuous photolysis in the presence of 0.1 M TEOA. [e] Medium is 0.2 M LiCl, 0.05 M *N*-ethylmorpholine, pH 8.1. [f] Medium is 0.2 M LiCl, 0.05 M *N*-ethylmorpholine, pH 8.3. [g] Medium is 0.10 M HCl, 0.10 M LiCl.

Scheme I

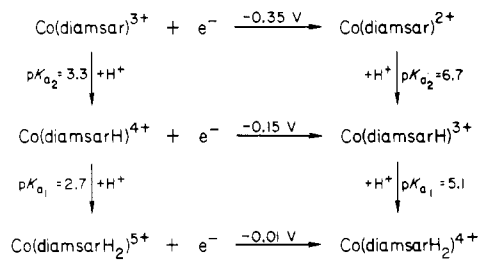

much slower stage the absorbance returns to its original value due to the reduction of RuL_3^{3+} by the $Co(cage)^{2+}$ species formed in equal concentration. The second-order rate constants k_t determined from the slower absorbance changes are listed in Table IV. A complication at neutral pH was the reduction of RuL_3^{3+} by the basic form of *N*-ethylmorpholine (B). The rate of this reaction ($k_{obsd}/[B] = 1.8 \times 10^6$, 1.2×10^6, and 3.4×10^5 M^{-1} s^{-1} for L = 5-Cl(phen), phen, and 4,7-$(CH_3)_2$phen, respectively, μ = 0.20 M (LiCl), 25 °C) was competitive with the $Co(cage)^{2+}$–RuL_3^{3+} back-reaction under standard flash photolysis conditions. In order to minimize the effect of the side-reaction, the back-reaction rate was increased by adding $(0.4–1.3) \times 10^{-3}$ M $Co(cage)^{2+}$: the back-reaction was pseudo first order under these conditions with a rate linearly dependent on the $Co(cage)^{2+}$ concentration. Another side-reaction on a slower time scale was the oxidation of the coordinated diamsar ligand as shown by the slow reaction of $Ru(bpy)_3^{3+}$ with $Co(diamsar)^{3+}$ ($k = 1.1 \times 10^3$ M^{-1} s^{-1}, 0.1 M phosphate, pH 7.5). By contrast, $Co(sep)^{3+}$ did not undergo any measurable reaction with $Ru(bpy)_3^{3+}$ (the very slow reaction observed in the latter system was due to the reaction of $Ru(bpy)_3^{3+}$ with solvent).

The $Co(diamsar)^{2+}$ complex is capable of adding two protons to the pendant amino groups. To ensure that the acidic forms of the complex were not involved in the back-reaction at pH ≥7.5, the pK_a values of the Co(III) and Co(II) complexes were estimated from the $E_{1/2}$ values (determined by cyclic voltammetry) measured at various pHs. The resulting pK_a's (to ± 0.3 pK_a unit) are summarized in Scheme I. These data indicate that at pH 1 and >7.5 the dominant forms of both the Co(III) and Co(II) complexes are the doubly protonated and unprotonated forms, respectively.

The yields of separated RuL_3^{3+} and $Co(cage)^{2+}$ produced in the quenching reactions, corrected for the fraction of

Scheme II

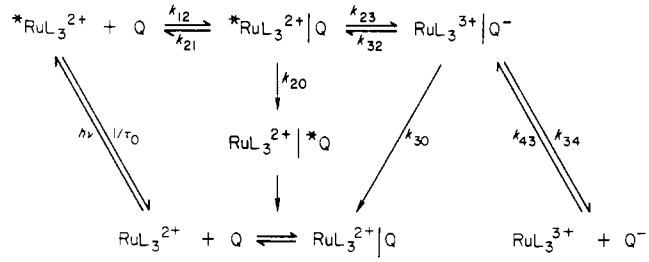

$*RuL_3^{2+}$ unquenched by $Co(cage)^{3+}$, are also included in Table IV. These yields were determined with the frequency-doubled Nd laser system (λ_{ex} = 530 nm).[17]

Discussion

Previous studies of quenching processes such as reaction 2 have implicated the detailed mechanism shown in Scheme II.[4,10,14] The reactants $*RuL_3^{2+}$ and Q first diffuse together to form a precursor complex. Energy transfer within the precursor complex ultimately yields ground-state RuL_3^{2+} and Q (either in the same solvent cage or separated, depending on the lifetime of Q*) while electron transfer within the precursor complex yields the successor complex in which RuL_3^{3+} and Q^- remain associated within the solvent cage. Diffusion from this solvent cage (dissociation of the successor complex) yields the separated electron-transfer products while electron transfer within the successor complex can either re-form the precursor complex or ground-state RuL_3^{2+} and Q. For this scheme a diffusion-corrected quenching rate constant k_{qc} can be defined by

$$1/k_q = 1/k_{12} + 1/k_{qc} \tag{4}$$

where k_{12} is the diffusion-controlled rate constant. If the energy-transfer path does not lead to electron-transfer products and if the quenching reaction is sufficiently exothermic so that the back-reaction to re-form the precursor complex can be neglected (i.e., $k_{32} \ll k_{30} + k_{34}$), then k_{qc} is equal to $k_{el} + k_{en}$ where $k_{el} = K_{12}k_{23}$, $k_{en} = K_{12}k_{20}$, $K_{12} = k_{12}/k_{21}$, and k_{el} and k_{en} are the (second-order diffusion-corrected) rate constants for the electron-transfer and energy-transfer paths, respectively; K_{12} is the equilibrium constant for the formation of the precursor complex. In terms of the semiclassical formalism,[4,18] the various parameters required for the calculation of k_{el} are given by eq 5–8, where r is the separation of the centers of

$$K_{12} = \frac{4\pi N r^2 \delta r}{1000} \exp(-w/RT) \tag{5}$$

$$w = \frac{z_1 z_2 e^2}{D_s r(1 + \beta r(\mu^{1/2}))} \tag{6}$$

$$k_{23} = \nu_{23}\kappa_{23} \exp(-\Delta G^*_{23}/RT) \tag{7}$$

$$\Delta G^*_{23} = (\Delta G^*_0)_{23}\left[1 + \frac{\Delta G^\circ_{23}}{4(\Delta G^*_0)_{23}}\right]^2 \tag{8}$$

the two reactants (11.3 Å), δr is the thickness of the reaction layer (0.8 Å), ν_{23} is an effective nuclear frequency (6×10^{12} s^{-1}), $(\Delta G^*_0)_{23}$ is the reorganization energy at zero driving force, and the other symbols have their usual significance.

(17) (a) Slightly larger yields were obtained with the dye-laser system (λ_{ex} = 440 nm). The latter yields needed to be corrected for the absorption of excitation light by the $Co(cage)^{3+}$ complexes and, more importantly, for "recycling" of RuL_3^{2+} during the relatively long laser pulse[17b] (0.6 μs for the dye laser vs. 25 ns for the Nd laser). For these reasons, the yields determined with the Nd laser are considered more reliable and only these are reported here. (b) Creutz, C.; Chou, M.; Netzel, T. L.; Okumura, M.; Sutin, N. *J. Am. Chem. Soc.* **1980**, 102, 1309.

(18) Sutin, N. *Acc. Chem. Res.* **1982**, *15*, 275. Sutin, N. *Prog. Inorg. Chem.* **1983**, *30*, 441.

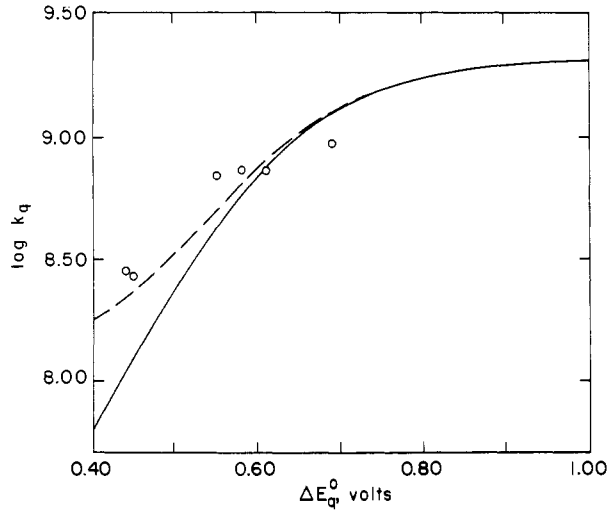

Figure 1. Plots of log k_q vs. ΔE_q° for the quenching of $^*RuL_3^{2+}$ emission (L = phen or substituted phen) by $Co(sep)^{3+}$ at 25 °C and 0.20 M LiCl. The curves were calculated by using $K_{12} = 0.2\ M^{-1}$, $k_{12} = k_{diff} = 2.2 \times 10^9\ M^{-1}\ s^{-1}$, $(\Delta G^*_0)_{23} = 0.43$ eV, and $\kappa = 1$ with $k_{en} = 0$ (solid curve) and $k_{en} = 1.3 \times 10^8\ M^{-1}\ s^{-1}$ (dashed curve).

In Figure 1 a plot of log k_q vs. $\Delta E_q^\circ (= -\Delta G^\circ_{23})$ for quenching of the emission of $Ru(phen)_3^{2+}$ and its derivatives by $Co(sep)^{3+}$ in 0.20 M LiCl (Table II) is presented. The solid curve was calculated from eq 4–8 by assuming $k_{en} = 0$ and using the following values of the other parameters: the value of $k_{12} = k_{diff}$ was taken as $2.2 \times 10^9\ M^{-1}\ s^{-1}$ (the rate constant for the reaction of $^*Ru(phen)_3^{2+}$ with $Ru(NH_3)_6^{3+}$ at 25 °C and 0.20 M LiCl), and $K_{12} = 0.2\ M^{-1}$ was calculated from eq 5 and 6. The electronic factor κ for the quenching (and self-exchange) reactions was taken as unity. A value of 0.43 eV for the reorganization energy at zero driving force was calculated from the self-exchange rates of the couples ($4 \times 10^8\ M^{-1}\ s^{-1}$ for the $^*RuL_3^{2+}$–RuL_3^{3+} and $5.1\ M^{-1}\ s^{-1}$ for the $Co(sep)^{3+}$–$Co(sep)^{2+}$ exchange). The agreement of the calculated and observed rate constants is satisfactory at high ΔE_q°, but the observed rate constants are consistently too large at lower ΔE_q°.[19] This behavior suggests that the energy-transfer path cannot be neglected, a conclusion also reached by Lay et al.[9] The dashed line in Figure 1 was calculated by using eq 4 with a free energy independent $k_{en} = 1.3 \times 10^8\ M^{-1}\ s^{-1}$ and the above values of the other parameters: the agreement with the observed quenching constants is improved considerably. Similar behavior was also found for quenching by $Co(azamesar)^{3+}$ and $Co(diamsar)^{3+}$: in each case the fit of the free energy dependence of the quenching rate constants could be improved by introducing a contribution from a free energy independent energy-transfer path ($k_{en} = 1.3 \times 10^8$ and $1.0 \times 10^8\ M^{-1}\ s^{-1}$, respectively).

The above interpretation is supported by the yields of the separated electron-transfer products. These yields may be expressed as the product of two factors (eq 9): the first factor

$$\Phi_{Ru(III),Co(II)} = f_q Y_{el} \tag{9}$$

$$f_q = \frac{K_{SV}[Q]}{1 + K_{SV}[Q]} \tag{10}$$

f_q is a correction for the fraction of excited states unquenched by Q, and the second factor Y_{el} is the efficiency of formation

(19) An exception is the quenching of the 3,5,6,8-$(CH_3)_4$phen complex in 0.50 M H_2SO_4 for which ΔE_q° is large (Table II), but which proceeds more slowly than predicted. This relatively slow quenching rate may reflect an enhanced nonadiabaticity of the quenching (or exchange) reaction: the increased nonadiabaticity must result from the presence of methyl groups in positions 5 and 6 of the tetramethyl derivative, since the quenching of the 3,4,7,8-$(CH_3)_4$phen complex appears "normal".

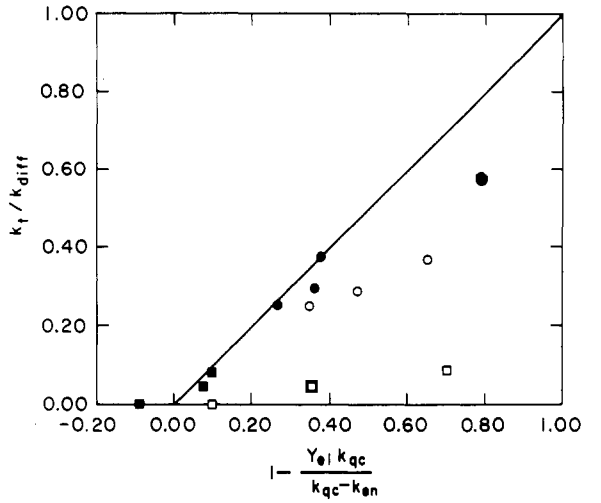

Figure 2. Plot of k_t/k_{diff} vs. $1 - Y_{el}k_{qc}/(k_{qc}-k_{en})$ for the quenching of $^*RuL_3^{2+}$ emission (L = phen or substituted phen) by $Co(cage)^{3+}$ and the back-reactions of RuL_3^{3+} with $Co(cage)^{2+}$ with $k_{diff} = 2.2 \times 10^9\ M^{-1}\ s^{-1}$: closed circles, $Co(sep)^{3+/2+}$, $k_{en} = 1.3 \times 10^8\ M^{-1}\ s^{-1}$; open circles, $Co(sep)^{3+/2+}$, $k_{en} = 0$; closed squares, $Co(diamsar)^{3+/2+}$, $k_{en} = 1.0 \times 10^8\ M^{-1}\ s^{-1}$; open squares, $Co(diamsar)^{3+/2+}$, $k_{en} = 0$. The solid line has the slope and intercept predicted by eq 14.

of separated electron-transfer products in the quenching reactions. In terms of Scheme II, Y_{el} is given by eq 11 and 12,

$$Y_{el} = \frac{k_{el}}{k_{qc}}\left[\frac{k_{34}}{k_{30} + k_{34}}\right] \tag{11}$$

$$Y_{el} = \frac{k_{el}}{k_{qc}}\Phi_{cage} \tag{12}$$

where $\Phi_{cage} = k_{34}/(k_{30} + k_{34})$ is the fraction of electron-transfer products that escape from the solvent cage in which they were formed. Recalling that k_t is given by eq 13 and that

$$k_t = \left[\frac{k_{30}k_{43}}{k_{30} + k_{34}}\right] \tag{13}$$

$k_{43} = k_{diff}$ and $k_{qc} = (k_{el} + k_{en})$, eq 14 can be derived from

$$\frac{k_t}{k_{diff}} = 1 - \frac{Y_{el}k_{qc}}{k_{qc} - k_{en}} \tag{14}$$

eq 12 and 13. The plot suggested by eq 14 is shown in Figure 2: the open points are for the case $k_{en} = 0$ and the solid points are for the k_{en} values implicated in the quenching studies. There is much better agreement of the data with eq 14 for the latter case, justifying the procedure used and providing further evidence for the presence of a modest quenching contribution from an energy-transfer pathway.

An interesting feature comes to light when the absolute values of k_t and Y_{el} are considered. The driving forces for the back-reactions are very large (Table IV) and, in terms of the above model, should result in $k_{30} \gg k_{34}$. As a consequence, the back-reaction rates should be diffusion controlled ($k_t \rightarrow k_{diff}$, see Figure 2) and the yields of separated electron-transfer products should be very low. Despite this prediction, k_t is significantly smaller than k_{diff} and the product yields are appreciable. This apparent anomaly can be understood if the back-reactions are nonadiabatic, that is, that $\kappa \ll 1$ for the reactions of RuL_3^{3+} with $Co(sep)^{2+}$ or $Co(diamsar)^{2+}$. If $\kappa \ll 1$, at high driving force k_t will equal $K_{12}\kappa\nu_n$ rather than k_{diff} ($k_{30} \rightarrow \kappa\nu_n$ rather than $k_{30} \rightarrow \nu_n$). In the present system the cage-escape yields implicate $\kappa \leq 1 \times 10^{-3}$ and $\leq 2 \times 10^{-4}$ for the $Co(sep)^{2+}$ and $Co(diamsar)^{2+}$ back-reactions, respectively. This conclusion receives strong support from the free energy dependence of the back-reaction rate constants (Figure 3).

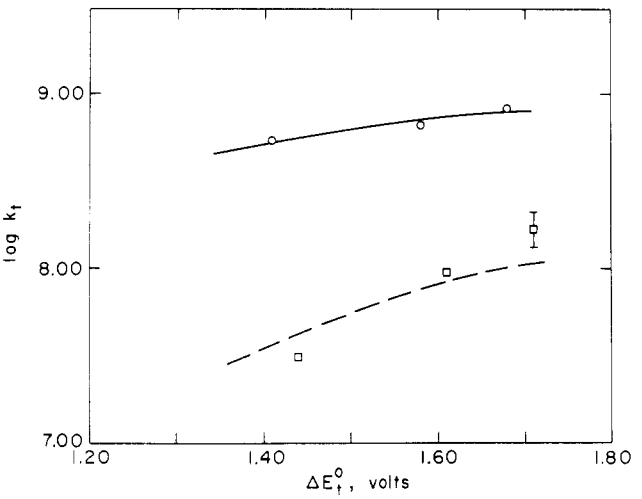

Figure 3. Plots of log k_t vs. ΔE_t° for the back-reaction of RuL_3^{3+} with $Co(sep)^{2+}$ (circles) and $Co(diamsar)^{2+}$ (squares). The solid curve was calculated from the same parameters as were used to fit the quenching data but with $\kappa = 1 \times 10^{-3}$. The dashed curve was similarly calculated with $\kappa = 2 \times 10^{-4}$.

The curve drawn through the $Co(sep)^{2+}$ data was calculated with the same parameters as were used to fit the free energy dependence of the $Co(sep)^{3+}$ quenching rate constants (Figure 1), but with $\kappa = 1 \times 10^{-3}$ for the back-reaction rather than with $\kappa = 1$ as used for the quenching reaction. Similarly, the curve through the $Co(diamsar)^{2+}$ data in Figure 3 was calculated by using $\kappa = 2 \times 10^{-4}$. In each case a satisfactory fit to the experimental data is obtained.[20]

The nonadiabaticity of the back-reactions is presumably a consequence of poor coupling of the RuL_3^{3+} and $Co(cage)^{2+}$ orbitals. Reactions of RuL_3^{3+} are frequently slower than predicted, and nonadiabaticity has been invoked as a possible reason for the slow rates.[10,14,21,22] It has also been proposed that the near-adiabaticity of other RuL_3^{3+} reactions derives from the enhanced electronic coupling resulting from the interpenetration of the coordination shells of the two reactants.[22] Since such interpenetration is not possible with the cage compounds, its absence could account for the nonadiabaticity of their reactions with RuL_3^{3+}. Interpenetration of the coordination shells of the reactants is expected to be less critical in oxidations of the RuL_3^{2+} excited state, since the promoted electron is located on the bipyridine ligands, and is consistent with the higher adiabaticity calculated for the quenching reactions.[23]

Comparisons with Other Systems. From the above considerations it is expected that reactions of the cobalt cage complexes with poly(pyridine) complexes in which the redox changes are metal centered should in general feature large nonadiabaticities. Consistent with this interpretation, the reaction of $Co(sep)^{2+}$ with $Co(phen)_3^{3+}$ ($k = 4.8 \times 10^3$ M^{-1} s^{-1} in 0.1 M Cl^-) proceeds about 100 times more slowly than predicted by an adiabatic model.[24] On the other hand, this prediction is not borne out in the reactions of $Co(sep)^{2+}$ with $Cr(bpy)_3^{3+}$ ($k = 2.3 \times 10^5$ M^{-1} s^{-1} in 0.2 M Cl^-) or with $Cr(5\text{-}CH_3(phen))_3^{3+}$ ($k = 2 \times 10^5$ M^{-1} s^{-1} in 0.1 M Cl^-)[25] —the rate constants for both reactions are consistent with $\kappa \sim 1$ (or at least with κ approximately equal to the square root of κ for the $Co(sep)^{3+/2+}$ exchange[18]). The CrL_3^{3+} reactions differ from the RuL_3^{3+} and $Co(phen)_3^{3+}$ reactions in at least two important respects: First, there are charge-transfer excited states[26] lying at lower energies in $CrL_3^{3+/2+}$ than in the corresponding ruthenium and cobalt couples; mixing of these states with the ground states to give a larger electronic coupling is likely to be more favorable for the CrL_3^{3+} reactions. Second, the CrL_3^{3+} reactions are close to thermoneutral, while the RuL_3^{3+} and $Co(phen)_3^{3+}$ reactions are highly exergonic (ΔE° = 1.41–1.68 and 0.68 V, respectively). An apparent dependence of the nonadiabaticity on the driving force for electron transfer has previously been noted,[21] and it is instructive to consider this further in the present context.

The electronic factor for a nonadiabatic reaction may vary with driving force for several reasons. The most likely source of such a driving-force dependence is mixing of electronically excited states: the electronic interaction between the reactant and product states increases as the excited-state energy decreases. For the purposes of discussion of the $Co(sep)^{2+}$–ML_3^{3+} reactions we consider the role of reactant excited states: the electronic interaction of the reactants, M^{III} and N^{II}, can be enhanced by mixing $^*\Psi(M^{III}N^{II})$, where either M^{III} or N^{II} is in an excited state, with the ground-state wave functions $\psi(M^{III}N^{II})$ and $\psi(M^{II}N^{III})$ for the reactants and products, respectively. Such mixing depends inversely upon ΔE^*, the vertical difference between the energy of the excited state and the energy of the ground state at the nuclear configuration corresponding to the intersection region (that is, at the intersection of the potential energy surfaces for the ground-state reactants and products). In a two-dimensional representation in which the surfaces are assumed to be harmonic and the equilibrium nuclear configuration of the excited surface is displaced relative to the reactants' surface minimum in the direction of the products' minimum, ΔE^* is given by

$$\Delta E^* = E_{CT} - \Delta G^* \left[1 - \frac{f_{CT}}{f}\right] - 2\left[\frac{f_{CT}}{f}\Delta G^*(E_{CT} - \Delta E_{CT}^\circ)\right]^{1/2} \quad (15)$$

where E_{CT} is the vertical difference between the energy of the excited state and the energy of the ground state at the equilibrium configuration of the ground state (the minimum in the reactants' potential energy surface), ΔE_{CT}° is the difference between the energies of the excited state and the reactants' ground state at their equilibrium configurations, and f_{CT} and f are the reduced force constants for the excited- and ground-state surfaces, respectively.[27] Evidently ΔE^* decreases

(20) (a) Although not required by the results, the data in Figure 1 can be accommodated to a nonadiabatic (quenching) reaction by postulating that the $Co(sep)^{3+/2+}$ exchange is less adiabatic than assumed. Decreasing the adiabaticity of the $Co(sep)^{3+/2+}$ exchange translates to a lower ΔG^*_0 for both the exchange and the quenching reactions; the latter in turn permits a lower κ for the quenching reaction. The degree of nonadiabaticity of the $Co(sep)^{3+/2+}$ exchange is still an open question: a calculation of the inner-shell reorganization energy considering only the difference in the metal–ligand bond lengths in the two oxidation states suggests $\kappa > 10^{-3}$ while a more extensive strain-energy calculation yields $\kappa = 10^{-4\pm2}$.[20b] Using $\kappa = 10^{-3}$ for the exchange give $(\Delta G^*_0)_{23}$ = 0.36 eV which, together with $k_{en} = 1.3 \times 10^8$ M^{-1} s^{-1} and $\kappa = 10^{-1}$ for the quenching reaction, yields a curve very similar to the dashed line in Figure 1. However, the back-reaction data (Figure 3) cannot be fit with smaller ΔG^*_0 values without reducing the free energy dependence of the rate constants. Although the free energy dependence can be restored by invoking additional free-energy-dependent reaction channels, this procedure seems rather arbitrary and, in any event, a much smaller adiabaticity would still be implicated for the back-reactions. (b) Endicott, J. F.; Brubaker, G. R.; Ramasami, T.; Kumar, K.; Dwarakanath, K.; Cassel, J.; Johnson, D. *Inorg. Chem.* **1983**, *22*, 3754.

(21) Chou, M.; Creutz, C.; Sutin, N. *J. Am. Chem. Soc.* **1977**, *99*, 5615.

(22) Macartney, D. H.; Sutin, N. *Inorg. Chem.* **1983**, *22*, 3530.

(23) The magnitudes of the electronic interaction matrix elements required to rationalize the nonadiabaticities of the quenching and back-reactions are approximately 30–100 and 3–10 cm^{-1}, respectively.[18]

(24) Endicott, J. F.; Ramasami, T.; Gaswick, D. C.; Tamilarasan, R.; Heeg, M. J.; Brubaker, G. R.; Pyke, S. C. *J. Am. Chem. Soc.* **1983**, *105*, 5301.

(25) (a) See ref 48 in: Brunschwig, B.; Sutin, N. *J. Am. Chem. Soc.* **1978**, *100*, 7568. (b) Ferraudi, G. I.; Endicott, J. F. *Inorg. Chim. Acta* **1979**, *37*, 219.

(26) (a) König, E.; Herzog, S. *J. Inorg. Nucl. Chem.* **1970**, *32*, 585. (b) Serpone, N.; Jamieson, M. A.; Emmi, S. S.; Fuochi, P. G.; Mulazzani, Q. G.; Hoffman, M. Z. *J. Am. Chem. Soc.* **1981**, *103*, 1091.

with decreasing E_{CT} and, provided $f_{CT} \leq f$, with decreasing driving force; i.e., as the driving force decreases, the intersection of the ground-state surfaces moves toward the products' minimum, thereby decreasing ΔE^* and increasing the electronic factor. For the RuL_3^{3+}, CoL_3^{3+}, and CrL_3^{3+} reactions with $Co(sep)^{2+}$ considered here, it appears that the net effect of mixing with excited states is to favor the CrL_3^{3+} reactions. Note that eq 15 reduces to

$$\Delta E^* = E_{CT} - 2[\Delta G^*(E_{CT} - \Delta E_{CT}^\circ)]^{1/2} \qquad (16)$$

when the force constants for the ground- and excited-state surfaces are the same and that the sign of the square root term changes on going from the normal to the inverted region.[28-30]

(27) The above expression (eq 15) differs from that reported recently[24] in that it does not assume that the minimum in the excited-state curve lies directly above the minimum in the products' potential energy surface. Reference 24 provides an elegant demonstration of the importance of charge-transfer interaction in the anion-catalyzed oxidation of $Co(sep)^{2+}$ by cobalt polypyridine complexes. Note that we have cast the arguments in terms of reactant excited states for the sake of conceptual simplicity. Similar considerations also apply to product excited states: the latter are likely to be the important ones in the CrL_3^{3+} reactions.

(28) In general, increasing the driving force will increase ΔE^*, thereby decreasing the electronic interaction energy H_{AB}. This dependence of H_{AB} on driving force will tend to decrease the free energy dependence of rates in the normal region. The situation is more complicated in the inverted region, where κ has a maximum value of $^1/_2$, beyond which it decreases again with increasing H_{AB}.[29] If H_{AB} is large, then κ will increase with decreasing H_{AB} (increasing driving force), thereby decreasing the free energy dependence of rates in the inverted region. On the other hand, if H_{AB} is small, then κ will decrease with decreasing H_{AB} (increasing driving force), thereby increasing the free energy dependence of rates in the inverted region.

(29) Newton, M. D.; Sutin, N. *Annu. Rev. Phys. Chem.*, in press.

(30) Even when the electronic interaction energy is independent of driving force, a driving-force-dependent electronic factor can still arise if $|\Delta E_0| > E_\lambda$ (where $|\Delta E_0| \sim |\Delta G^\circ|$ and $E_\lambda \sim 4\Delta G^*_0$). This occurs through the coefficient that relates κ to the electronic interaction energy. In the high-temperature limit ($h\nu < kT$) the electronic factor is proportional to $1/(E_\lambda RT)^{1/2}$, which is independent of driving force. On the other hand at low temperatures ($h\nu > kT$) and $|\Delta E_0| > E_\lambda$, the electronic factor is proportional to $1/(|\Delta E_0|h\nu)^{1/2}$, which decreases with increasing driving force. The RuL_3^{3+} reactions considered here are in the barrierless region ($|\Delta E_0| \sim E_\lambda$) where it is difficult to assess the importance of this effect. In general, larger κ variations may be anticipated from the first effect considered, especially when the excited states are relatively low lying.

Conclusions. The quenching of $*RuL_3^{2+}$ emission by cobalt(III) cage compounds proceeds by parallel electron-transfer and energy-transfer paths, with the former predominating at high driving force. The free energy dependence of the quenching and back-reaction rate constants can be accounted for in terms of the weak-interaction semiclassical model with $\kappa \sim 1$ for the quenching reactions and $\kappa = 10^{-3}$–10^{-4} for the back-reactions. The relatively large yields of separated electron-transfer products observed in these systems are a consequence of the nonadiabaticity of the back-reactions. Mixing of ground-state and excited-state wave functions seems to be important in the reactions of the cage compounds with tris(bipyridine) complexes. The possibility that the electronic factor is driving-force dependent should be kept in mind in analyzing the free energy dependence of the rates in the normal and inverted regions.

Acknowledgment. We thank Dr. B. S. Brunschwig for helpful discussions and for assistance with some of the flash photolysis measurements, Dr. S. Isied for suggesting the procedure for separating RuL_3^{2+} and $Co(sep)^{3+}$, and Dr. D. H. Macartney for measuring the $Co(sep)^{2+}$–$Cr(bpy)_3^{3+}$ rate. C.-Y.M. and A.W.Z. were on sabbatical leave from the National University of Singapore, Singapore, and Claremont College, CA, respectively. This work was performed at Brookhaven National Laboratory under contract with the U.S. Department of Energy and supported by its Office of Basic Energy Sciences.

Registry No. TEOA, 102-71-6; MV^{2+}, 4685-14-7; $Ru(bpy)_3^{2+}$, 15158-62-0; $Ru(4,4'\text{-}(CH_3)_2bpy)_3^{2+}$, 32881-03-1; $Ru(5\text{-}Br(phen))_3^{2+}$, 66908-45-0; $Ru(5\text{-}Cl(phen))_3^{2+}$, 47860-47-9; $Ru(phen)_3^{2+}$, 22873-66-1; $Ru(5\text{-}(CH_3)phen)_3^{2+}$, 14975-39-4; $Ru(5,6\text{-}(CH_3)_2phen)_3^{2+}$, 14975-40-7; $Ru(4,7\text{-}(CH_3)_2phen)_3^{2+}$, 24414-00-4; $Ru(3,5,6,8\text{-}(CH_3)_4phen)_3^{2+}$, 14781-17-0; $Ru(3,4,7,8\text{-}(CH_3)_4phen)_3^{2+}$, 64894-64-0; $Co(sep)^{3+}$, 72496-77-6; $Co(diamsar)^{3+}$, 85663-96-3; $Co(diamsarH)^{4+}$, 90624-02-5; $Co(diamsarH_2)^{5+}$, 85663-73-6; $Co(azamesar)^{3+}$, 85664-08-0; $Co(ammesarH)^{4+}$, 85664-45-5; $Ru(5\text{-}Cl(phen))_3^{3+}$, 79736-56-4; $Ru(phen)_3^{3+}$, 23633-32-1; $Ru(4,7\text{-}(CH_3)_2phen)_3^{3+}$, 79747-03-8; $Ru(bpy)_3^{3+}$, 18955-01-6; $Co(sep)^{2+}$, 63218-22-4; $Co(diamsar)^{2+}$, 72560-63-5; $Co(diamsarH_2)^{4+}$, 85664-44-4.